Molecular Microbiology (2015) 98(4), 727–742 ■
doi:10.1111/mmi.13152
First published online 10 September 2015

The role of FlhF and HubP as polar landmark proteins in *Shewanella putrefaciens* CN-32

Florian Rossmann,[1,2†] Susanne Brenzinger,[1,2†] Carina Knauer,[3] Anja K. Dörrich,[1] Sebastian Bubendorfer,[1‡] Ulrike Ruppert,[1] Gert Bange[3] and Kai M. Thormann[1*]

[1]*Department of Microbiology and Molecular Biology, Justus-Liebig Universität, 35392 Giessen, Germany.*
[2]*Department of Ecophysiology, Max-Planck-Institut für terrestrische Mikrobiologie, 35043 Marburg, Germany.*
[3]*LOEWE Center for Synthetic Microbiology (Synmikro) & Department of Chemistry, Philipps University Marburg, 35043 Marburg, Germany.*

Summary

Spatiotemporal regulation of cell polarity plays a role in many fundamental processes in bacteria and often relies on 'landmark' proteins which recruit the corresponding clients to their designated position. Here, we explored the localization of two multi-protein complexes, the polar flagellar motor and the chemotaxis array, in *Shewanella putrefaciens* CN-32. We demonstrate that polar positioning of the flagellar system, but not of the chemotaxis system, depends on the GTPase FlhF. In contrast, the chemotaxis array is recruited by a transmembrane protein which we identified as the functional ortholog of *Vibrio cholerae* HubP. Mediated by its periplasmic N-terminal LysM domain, *Sp*HubP exhibits an FlhF-independent localization pattern during cell cycle similar to its *Vibrio* counterpart and also has a role in proper chromosome segregation. In addition, while not affecting flagellar positioning, *Sp*HubP is crucial for normal flagellar function and is involved in type IV pili-mediated twitching motility. We hypothesize that a group of HubP/FimV homologs, characterized by a rather conserved N-terminal periplasmic section required for polar targeting and a highly variable acidic cytoplasmic part, primarily mediating recruitment of client proteins, serves as polar markers in various bacterial species with respect to different cellular functions.

Accepted 30 July, 2015. *For correspondence. E-mail kai.thormann@mikro.bio.uni-giessen.de; Tel. +49 (0) 641 9935545; Fax +49 (0)641 9935549. †These authors contributed equally to this study. ‡Present address: Institute for Medical Microbiology and Hospital Epidemiology, Hannover Medical School, Hannover 30625, Germany.

Introduction

During the recent decades, numerous studies have provided evidence that in bacteria, a variety of fundamental cellular functions depend on the proper spatial and temporal organization of proteins and other macromolecules within the cell. A paradigmatic example for spatiotemporal organization in bacteria is cell division where correct positioning of the cell division proteins and distribution of replicated chromosomal DNA are critical for propagation (Thanbichler, 2010; Reyes-Lamothe *et al.*, 2012). Unlike the cell division machinery of most bacteria, numerous other complexes are specifically targeted to the cell pole for proper function. Several different systems involved in the regulation of cell polarity have been identified and studied; this topic has been the subject of recent reviews (Laloux and Jacobs-Wagner, 2014; Treuner-Lange and Søgaard-Andersen, 2014).

One major multiprotein complex that needs to be specifically positioned is the flagellar machinery of polarly flagellated bacterial species. The mechanisms by which this localization is achieved are still poorly understood for most bacteria (summarized in Schuhmacher *et al.*, 2015a). In those species that have been studied in detail, polar recruitment of the flagellar system appears to rely on landmark proteins to assign the desired position, and the absence of these polar markers commonly leads to misplacement of the flagella. In the alphaproteobacterium *Caulobacter crescentus*, TipN has been identified as such a landmark protein (Huitema *et al.*, 2006; Lam *et al.*, 2006). TipN localizes to the new pole of both daughter cells after cell division and recruits a second protein, TipF, a positive regulator of flagellar assembly. TipF in turn recruits PflI, a third protein required for proper flagellar placement (Obuchowski and Jacobs-Wagner, 2008; Davis *et al.*, 2013). The concerted action of these three proteins is required for formation of a single flagellum at the designated cell pole (Davis *et al.*, 2013).

However, homologs of the TipN/F proteins appear to be absent outside the group of alphaproteobacteria. In many other bacterial species, a set of two proteins, FlhF and FlhG, has been implicated in regulating diverse aspects of

flagellar localization, number, and activity (reviewed in Kazmierczak and Hendrixson, 2013; Altegoer *et al*., 2014). Potential orthologs of the two proteins are present in a wide range of bacterial species (Bange *et al*., 2011). FlhG (orthologs also named YlxH, MinD2, FleN or MotR) belongs to the MinD/ParA ATPase family, and the recently solved crystal structure revealed striking structural homologies to the ATPase MinD of *Escherichia coli* (Schuhmacher *et al*., 2015b). Loss of FlhG in polarly flagellated bacterial species commonly results in hyperflagellation and severe perturbation of flagella-mediated motility (Dasgupta *et al*., 2000; Correa *et al*., 2005; Kusumoto *et al*., 2006; 2008; Schuhmacher *et al*., 2015b). The exact mechanism by which FlhG exerts its role is still elusive; however, its mode of action involves binding to major components of the flagellar rotor, FliM and FliN/FliY, putatively to facilitate their incorporation into the nascent basal body structure (Schuhmacher *et al*., 2015b). The second protein of the system, FlhF, belongs to the signal recognition particle SRP-type GTPase subfamily of the SIMIBI class of nucleotide-binding proteins, and the crystal structure of FlhF from *Bacillus subtilis* has been solved (Bange *et al*., 2007; Bange and Sinning, 2013). Loss of the protein has a range of different consequences with respect to flagellar gene expression, assembly and function in various polarly flagellated species, but consistently results in displacement of the flagellum away from the cell pole (Pandza *et al*., 2000; Murray and Kazmierczak, 2006; Kusumoto *et al*., 2008; Balaban *et al*., 2009; Green *et al*., 2009). FlhF was demonstrated to co-localize with the flagellum to the old cell pole (Murray and Kazmierczak, 2006; Kusumoto *et al*., 2008; Ewing *et al*., 2009). Moreover, studies on *Vibrio cholerae* FlhF have provided evidence that the same spatial organization occurs in the absence of any other flagellar components (Green *et al*., 2009) or upon heterologous production of *Vibrio alginolyticus* FlhF in *E. coli* (Kusumoto *et al*., 2008), indicating that polar localization is an intrinsic feature of the protein. The presence of FlhF at the cell pole is required for correct placement of the early flagellar basal body protein FliF. Thus, it has been speculated that FlhF represents the polar landmark protein which recruits early components of the flagellar machinery to the appropriate subcellular location by a mechanism which is yet elusive. In addition, for *Pseudomonas aeruginosa*, it was reported that the chemotaxis protein CheA also localizes away from the cell pole in the absence of FlhF in a pattern resembling that of the flagellar basal body system (Kulasekara *et al*., 2013). This finding strongly indicates that FlhF might also mediate the recruitment of the chemotaxis machinery in *P. aeruginosa* or that the chemotaxis machinery is directly associated with the flagellar system.

Recent studies on *V. cholerae* have identified another major landmark protein which is involved in the polar accumulation of flagella but primarily directs the chemotaxis system and the chromosome segregation machinery to the cell pole. According to its proposed function as a polar hub, the protein was named HubP (Yamaichi *et al*., 2012). HubP is a transmembrane protein with an N-terminal periplasmic peptidoglycan-binding (LysM) domain and a large cytoplasmic section comprising 10 copies of an imperfect 46-amino-acid repeat. Fluorescence microscopy demonstrated that, mediated by the N-terminal LysM domain, HubP localizes to the cell pole and the cellular division plane. Deletion of *hubP* in *V. cholerae* results in delocalization of the chemotaxis machinery, leading to a defect in chemotactic swimming. In addition, the origin of the larger of the two *V. cholerae* chromosomes, *oriCI*, is not fully targeted to the cell pole and a small fraction of cells displays an increased number of flagella. Interaction of these large complexes with HubP is thought to be mediated through a set of different ParA-like ATPases, ParAI for *oriCI*, ParC for the chemotaxis machinery and FlhG for the flagellar machinery. Potential homologs of HubP have been identified in several other species among the gammaproteobacteria; however, it is not clear whether or not these proteins are functional orthologs and which role they might play in these species.

Shewanella putrefaciens CN-32 is a gammaproteobacterium which possesses two complete flagellar systems encoded by two distinct separate gene clusters (Bubendorfer *et al*., 2012). The primary gene cluster, which is present in all *Shewanella* species and encodes orthologs of FlhF and FlhG, leads to formation of a single polar Na^+-driven flagellum. The secondary flagellar system lacks *flhF* and *flhG* and is expressed in a subpopulation of cells when cultivated in complex media. These cells form one or more lateral flagella which are rotated at the expense of the proton gradient and enable a more effective motility of the corresponding subpopulation by increasing the directional persistence of swimming. However, our studies strongly indicated that the single chemotaxis system of *S. putrefaciens* CN-32 predominantly or even exclusively addresses the primary polar system but not the lateral flagellar motors (Bubendorfer *et al*., 2014). To further elucidate the spatial arrangement of the chemotaxis machinery with respect to the two flagellar systems of *S. putrefaciens* CN-32, we performed localization studies by fluorescence microscopy. We identified the functional ortholog of the *V. cholerae* polar landmark protein HubP in *S. putrefaciens* CN-32, and we demonstrate that FlhF and HubP independently localize the primary flagellar system and the chemotaxis and chromosome segregation machinery, respectively. We thus show that general features and mechanisms are conserved between HubP-like proteins of different species and suggest that HubP-dependent polar localization might be more widespread among bacteria.

Results

The chemotaxis machinery of S. putrefaciens *CN-32 localizes to the flagellated cell pole*

To first explore the subcellular position of the chemotaxis system in *S. putrefaciens* CN-32, we performed fluorescence microscopy on cells producing fluorescently labeled components of the chemotaxis machinery. *S. putrefaciens* CN-32 possesses a single chemotaxis system with 37 predicted putative methyl-accepting sensor proteins (MCPs). To determine the localization of the chemotaxis machinery within CN-32 cells, we generated C-terminal fluorescent protein fusions to 16 of the 37 MCPs. Because all fusions yielded very similar results, we will, within this manuscript, only refer to MCP0796-eGFP. MCP0796 is an MCP with a periplasmic helical bimodular (HBM) sensor domain followed by the typical cytoplasmic HAMP and methyl-accepting chemotaxis-like (MA) domain. The function of this MCP is not yet characterized; however, the fluorescent fusion reliably allowed localization of the protein which was therefore chosen as representative. We further generated a C-terminal fluorescent fusion to CheA (CheA-mCherry) as well as N-terminal fluorescent protein fusions to CheY (sfGFP-CheY) and CheZ (Venus-CheZ). The genes encoding these fusions were separately introduced into the CN-32 chromosome where they replaced the corresponding native genes. Immunoblotting and swimming assays demonstrated that the fluorescently labeled proteins were mostly stably produced (Fig. S1) and fully (Venus-CheZ and CheA-mCherry) or partially (sfGFP-CheY) supported movement through soft agar (Fig. S2). To enable localization of the chemotaxis machinery with respect to the position of the primary polar flagellar system, all fusions were introduced into a CN-32 strain in which $FliM_1$ was functionally labeled with sfGFP or mCherry (Bubendorfer *et al.*, 2012) as a marker for the primary basal body complex.

Subsequent fluorescence microscopy revealed that MCP0769-eGFP as well as sfGFP-CheY, CheA-mCherry and Venus-CheZ distinctly localized to the cell pole marked by $FliM_1$ in 73% (CheY and CheA) and 89% (CheZ) respectively (Fig. 1). In addition, some cells displayed a bipolar localization pattern of labeled chemotaxis components (CheY, 19%; CheA, 29%; CheZ, 21%). In cells with a $FliM_1$ focus, the signal intensity of co-localizing foci formed by the labeled chemotaxis components was always stronger than that of foci at the opposite cell pole: For sfGFP-CheY, the signal at the opposite cell poles only reached 38% intensity compared to that of the flagellated pole, CheA-mCherry reached 27% and Venus-CheZ 24%. In contrast, co-localization of any of the labeled chemotaxis components with $FliM_2$-mCherry as a marker for the position of the secondary lateral flagellum was not observed, unless $FliM_2$-mCherry was located close to the cell pole (data not shown). Based on these results, we concluded that in *S. putrefaciens* CN-32, the chemotaxis machinery is localized at, or in close proximity to, the cell pole decorated with the primary flagellar complex and is assembled at the old cell pole during cell division.

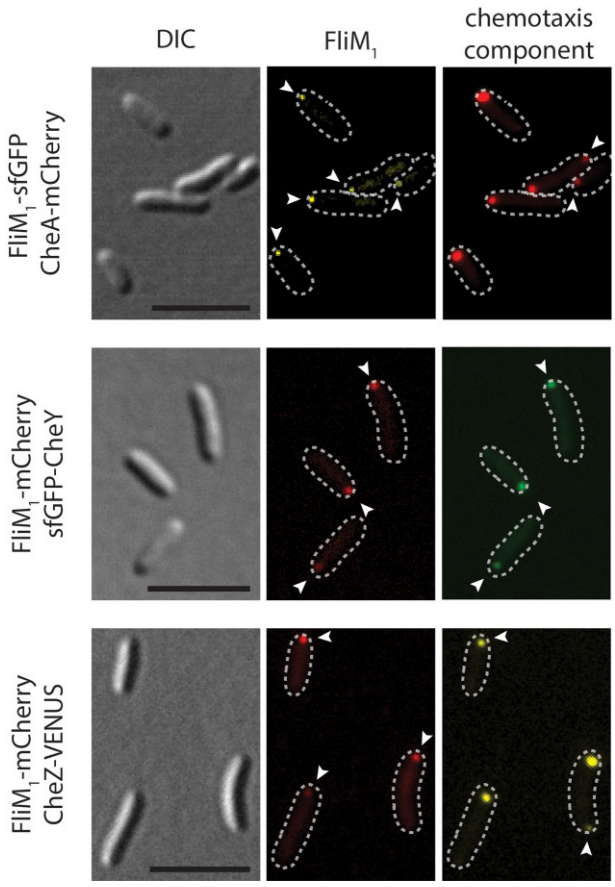

Fig. 1. Localization of the chemotaxis cluster in *S. putrefaciens* CN-32. Displayed are DIC (left panel) and fluorescent micrographs in which $FliM_1$ (middle panels) and CheA, CheY and CheZ (right panel) are fluorescently labeled as indicated. The arrows point out fluorescent foci. The scale bar equals 5 μm.

The SRP-like GTPase FlhF is required for polar localization of the primary flagellar system, but not of the chemotaxis cluster, in CN-32

The SRP-like GTPase FlhF has been demonstrated to be the major determinant for flagellar placement and number in various polarly flagellated gammaproteobacteria. We therefore determined whether this protein has a similar role in *S. putrefaciens* CN-32 and whether *Sp*FlhF also dictates the localization of the chemotaxis system, as has previously been suggested for *P. aeruginosa* (Kulasekara *et al.*, 2013). FlhF acts in concert with its antagonist, the MinD-like ATPase FlhG (Kusumoto *et al.*, 2008; Ono *et al.*, 2015), and in *B. subtilis* it has been shown that the conserved N-terminal region of FlhG stimulates the

GTPase activity of FlhF by approximately three to fivefold (Bange *et al.*, 2011). To assess whether FlhF from *S. putrefaciens* CN-32 is an active GTPase whose activity is affected by FlhG, both proteins were purified and the impact of *Sp*FlhG on the GTPase activity of *Sp*FlhF was assessed by high-pressure liquid chromatography (HPLC). While SpFlhF alone showed only minor GTPase activity, an approximately three to fivefold stimulation of SpFlhF was observed in the presence of either full-length FlhG or its N-terminal region. As expected, this stimulation was almost abolished in a GTP hydrolysis-deficient FlhF variant (FlhF-R285A; Fig. 2A). This agrees with observations made for FlhF and FlhG from *B. subtilis*. Correspondingly, an *flhG-ΔN20* mutant in CN-32 displayed a hyperflagellated phenotype (Fig. S3B) which was drastically impaired in flagella-mediated motility similar to a cell completely lacking *flhG* (Fig. S3A). This indicates that FlhG may also stimulate the FlhF GTPase in polarly flagellated gammaproteobacteria such as *S. putrefaciens* CN-32 and that this interaction likely is required for proper flagellation.

To localize *Sp*FlhF within the cells, we created a hybrid gene encoding a C-terminal fusion of FlhF to mCherry (*flhF-mCherry*) which we integrated into the chromosome to replace native *flhF*. FlhF-mCherry was partially stable (Fig. S1) and predominantly localized to the flagellated cell pole in 85% of the population (Fig. 2B). A bipolar localization frequently occurred in cells that evidently were within the process of cell division. To further determine whether FlhF has a function in regulating flagellar placement and number, we studied the localization of $FliM_1$ and the flagellar filament in the absence of *flhF*. To this end, we introduced in-frame deletions of *flhF* into CN-32 wild-type cells and into cells bearing a $FliM_1$-sfGFP fusion. To specifically enable visualization of the primary flagellum, cysteine residues were introduced in both flagellins forming the primary flagellar filament to enable fluorescent labeling ($FlaAB_1$-Cys) in the wild-type and *ΔflhF* background. In mutants lacking FlhF (*ΔflhF*), we observed a significantly lower amount of cells exhibiting $FliM_1$-mCherry foci (wild type, 72%; *ΔflhF*, 27%), and these foci were commonly displaced from the cell pole to lateral positions (Fig. 2D). Fluorescence labeling of the flagellins confirmed that, in the relatively few flagellated *ΔflhF* cells, the filament frequently originated from lateral positions. Significantly fewer cells were observed to be motile, and cells exhibited irregular swimming patterns when observed by light microscopy and decreased lateral extension when moving through soft-agar plates (Fig. 2C). When FlhF or FlhF-mCherry was ectopically overproduced from an inducible promoter in wild-type cells, we observed increased accumulation at the cell pole accompanied by hyperflagellation of the cells which solely occurred at the same cell pole (Fig. S4B). In contrast, deletion of *flhF* had no significant effect on the production or placement of the secondary filaments (Fig. S4C). We then determined the localization of MCP0796, CheY, CheA or CheZ in the absence of FlhF to explore potential effects on the localization of any of the fluorescently labeled components. In contrast to the primary flagellar system, all chemotaxis components retained a polar localization pattern indistinguishable from that observed in the wild-type background (Fig. 2D; Fig. S5).

We thus confirmed that, in *S. putrefaciens* CN-32, FlhF is an active GTPase that shares the common features and properties which have been described for other species of the gammaproteobacteria and serves as a polar landmark protein and regulator for polar flagellar assembly. Furthermore, we showed that FlhF does not direct the chemotaxis system to the flagellated cell pole, which prompted us to screen for other potential landmark proteins that might be required for cell polarity in *Shewanella*.

Shewanella *sp. possess a HubP ortholog*

In *V. cholerae*, polar localization of the chemotaxis machinery was recently demonstrated to be dependent on the transmembrane landmark protein HubP. Genome analysis revealed that HubP showed significant similarities to Sputcn32_2442, a gene of 3294 bp, predicted to encode a protein of 1097 aa. Sputcn32_2442 was preliminary annotated as pilus assembly protein FimV based on its similarity to *P. aeruginosa* FimV, a protein regulating cell polarity during type IV pili-mediated twitching motility (Semmler *et al.*, 2000; Wehbi *et al.*, 2011). However, at the amino-acid level, significant identity or similarity between Sputcn32_2442, *Vibrio* HubP or *P. aeruginosa* FimV was only observed for the N- and very C-terminal segments of the deduced protein sequence (Fig. S6). Despite the rather low overall similarity and a lower molecular mass (estimated 117 kDa compared with ~ 178 kDa of HubP), the predicted protein exhibited striking similarities to *Vibrio* HubP with respect to domain architecture and some other features (Fig. S7). Both Sputcn32_2442 and *Vibrio* HubP are highly acidic proteins (pI 3.87 and 3.22 respectively). Similar to HubP, Sputcn32_2442 is predicted to possess an N-terminal signal sequence (likely to be cleaved between aa 24 and 25) followed by a putative LysM peptidoglycan-binding domain and a transmembrane domain. Sputcn32_2442 is annotated to directly begin with the signal sequence, while *Vc*HubP features a short cytoplasmic stretch of amino acids prior to the rather hydrophobic residues. Both proteins harbor within their cytoplasmic C-terminal segment a number of copies of an imperfect repeat that is highly enriched in acidic amino acids (10 in *Vc*HubP; 9 in Sputcn32_2442). With a length of 37 aa, these repeats are shorter in Sputcn32_2442 than in *Vc*HubP (46 aa) and are also less well conserved.

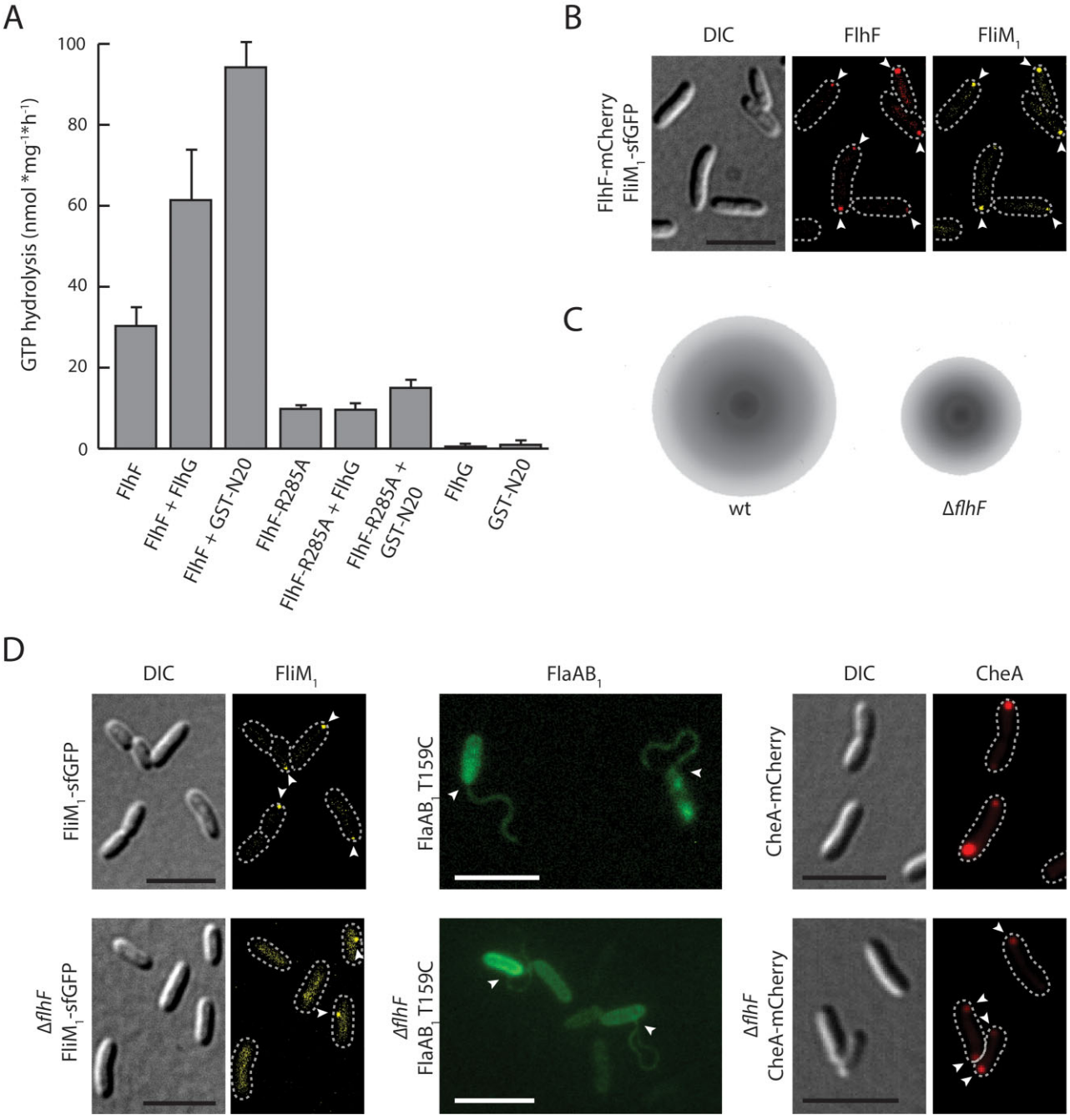

Fig. 2. Activity and role of FlhF in flagellar placement.
A. The GTPase activity of FlhF is stimulated by the N-terminus of FlhG. GTP hydrolysis in nmol per mg FlhF per hour is given as mean value ± standard deviation of three independent measurements.
B. FlhF localizes to the flagellated cell pole. Shown are DIC (left) and corresponding fluorescence micrographs of cells harboring fluorescent fusions to both FlhF and $FliM_1$ as indicated (right).
C. Loss of FlhF results in decreased swimming abilities in soft agar. 3 µl of exponentially growing cultures of the indicated strain were placed on 0.25% soft agar plates and incubated at 30°C for 16 h. Please note that the complete soft agar plate is displayed in Fig. S2.
D. FlhF has a role in localization of flagellar but not of chemotaxis components. In wild-type cells (upper panel), $FliM_1$, the flagellar filaments and CheA occur at the cell pole. In the absence of FlhF (lower panel), both $FliM_1$ and flagellar filaments are shifted to lateral positions. In contrast, chemotaxis components, here CheA, still occur at the cell poles. Displayed are DIC and fluorescent images in which the FlhF, $FliM_1$, CheA or the flagellins are fluorescently labeled (FlhF-mCherry; $FliM_1$-sfGFP, CheA-mCherry, Alexa-Fluor 488). Arrows mark fluorescent clusters and the positions of the flagellar filaments' origins respectively. The scale bar equals 5 µm.

With respect to the genetic context, both *hubP* and Sputcn32_2442 are flanked downstream by *truA*, a gene predicted to encode tRNA pseudouridine synthase A. Potential orthologs to Sputcn32_2442 can be readily identified in many other sequenced *Shewanella* species, but these exhibit variations in protein length and similarity particularly within the repeat domain of the protein (Fig. S7). Based on the similarities, and despite the low overall conservation at protein level, we hypothesized that Sputcn32_2442, henceforth *Sp*HubP, represents the functional ortholog of *Vc*HubP.

Sp*HubP localizes the chemotaxis, but not the flagellar system, to the cell pole*

In *V. cholerae*, HubP has been demonstrated to mediate polar localization of the chemotaxis cluster and to be involved in restricting the number of polar flagella to a single filament. To determine whether this similarly applies to *Sp*HubP, corresponding fluorescent protein fusions to $FliM_1$, MCP0976 (Sputcn32_0796-eGFP), CheY (sfGFP-CheY), CheA (CheY-mCherry) and CheZ (Venus-CheZ) were introduced into the CN-32 *ΔhubP* background and their localization was analyzed by fluorescence microscopy (Fig. 3A; Fig. S8A). We observed that, in the absence of *Sp*HubP, $FliM_1$-sfGFP exclusively remained at the pole in all cells. In addition, fluorescence labeling of the flagellar filament in *ΔhubP*-mutants revealed that the cells still displayed a single polar filament undistinguishable from the wild type. However, the number of cells with polar $FliM_1$-sfGFP clusters dropped significantly in the absence of *Sp*HubP (wild type, 72%; *ΔhubP*, 42%), and, accordingly, the number of flagellated cells was correspondingly lower. In contrast to the flagellar system, components of the chemotaxis machinery were no longer restricted to the cell pole but also localized to lateral positions within the cell envelope (Fig. 3A; Fig. S8A).

We also analyzed the major determinants for polar flagellar localization and number, FlhF and FlhG, in the CN-32 *ΔhubP* background (Fig. 3B; Fig. S8B). Polar positioning of FlhF occurred independently of *Sp*HubP as FlhF-mCherry exclusively localized in distinct clusters to the cell poles in both wild-type and the *ΔhubP*-mutant cells. However, as already observed with $FliM_1$-sfGFP, the frequency of cells displaying polar FlhF-mCherry foci dropped significantly in a population of cells lacking *Sp*HubP (wild type, 73%; *ΔhubP*, 46%). As previously observed in *Vibrio* species (Kusumoto *et al.*, 2008; Yamaichi *et al.*, 2012; Ono *et al.*, 2015), stable and fully functional FlhG-sfGFP displayed a cytoplasmic localization but also accumulated at the flagellated pole in a number of cells (51%). These discrete polar foci were virtually absent in a *ΔhubP* mutant (0.25%), strongly suggesting that polar localization of FlhG depends on *Sp*HubP as has previously been observed in *V. cholerae* (Yamaichi *et al.*, 2012). Taken together, the results strongly indicate that localization of the chemotaxis cluster is exclusively conferred by *Sp*HubP. Positioning of the polar flagellar system is primarily dictated by FlhF/FlhG; however, *Sp*HubP directly or indirectly affects the amount of polar accumulation of FlhF and FlhG and the size of the cellular subpopulation forming a flagellum.

The absence of Sp*HubP negatively affects motility*

To further determine whether *Sp*HubP might have a direct or indirect effect on the flagellar function, we analyzed the swimming behavior of cells by soft-agar assays and light microscopy (Fig. 4A and B). When placed on soft agar, the *ΔhubP* mutant displayed a significantly lower lateral extension than wild-type cells, indicating a decreased chemotactic drift and/or slower swimming. Analysis of cellular swimming by light microscopy revealed that *ΔhubP* mutant cells, in fact, exhibit a significant decrease in average swimming speed (wild type: 52.7 μm s^{-1}; *ΔhubP*: 29.5 μm s^{-1}). Such a phenotype has not been described for *Vc*HubP before and indicates that *Sp*HubP has further functions in motor performance in addition to ensuring close proximity between the chemotaxis and flagellar motor system.

Because the potential homolog of *Vc*- and *Sp*HubP in *P. aeruginosa*, FimV, is required for normal twitching motility (Semmler *et al.*, 2000; Wehbi *et al.*, 2011), we also determined type IV pili-mediated twitching motility of *S. putrefaciens* CN-32 wild-type and *ΔhubP* mutant cells. Although this type of movement was not very pronounced under the conditions tested, cells lacking *Sp*HubP showed a significant reduction in the area covered by twitching by a factor of about 4 (Fig. 4C).

Taken together, the results provide evidence that *Sp*HubP has different functions with respect to various aspects of motility in *S. putrefaciens* CN-32.

Sp*HubP has a complex localization pattern in* S. putrefaciens *CN-32*

To determine the localization of *Sp*HubP in *S. putrefaciens* CN-32 cells, we constructed a hybrid gene encoding a C-terminal fusion to sfGFP or mCherry, which we integrated into the chromosome to replace the native *hubP*. Immunoblotting analysis confirmed that *Sp*HubP-sfGFP and *Sp*HubP–mCherry were stably produced, and swimming analysis indicated that the labeled proteins were fully functional (Figs S1 and S2). Fluorescence microscopy revealed that *Sp*HubP-sfGFP mainly co-localizes with $FliM_1$-mCherry to the flagellated cell pole (Fig. 5A). The majority of cells (95%) also displayed minor fluorescence foci at the opposite pole with about half the intensity (47%) of that of the main cluster. In addition, in cells which were in the process of dividing, *Sp*HubP-mCherry was

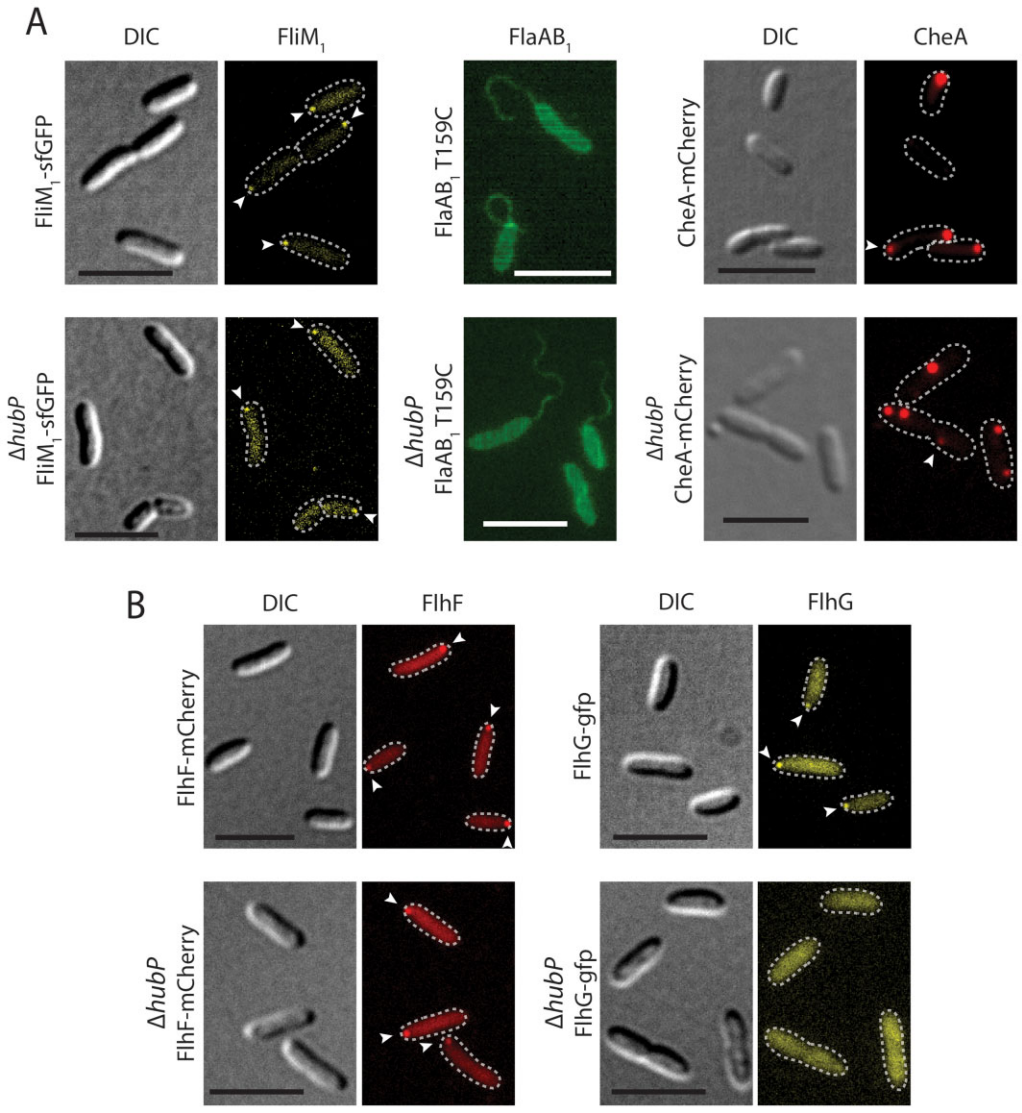

Fig. 3. Localization of flagellar and chemotaxis components in dependence of *Sp*HubP.
A. In the absence of *Sp*HubP, $FliM_1$ and flagellar filaments remain at the cell pole, while chemotaxis components, such as CheA, are delocalized to subpolar positions.
B. In the presence of *Sp*HubP, both FlhF and FlhG occur at the cell pole (upper panels, the corresponding line scan analysis can be found in Fig. S8). In *ΔhubP*-mutant cells (lower panel), FlhF remains at the cell pole while FlhG loses its polar accumulation pattern. Displayed are DIC and fluorescent micrographs in which $FliM_1$, CheA and the flagellar filament are appropriately labeled ($FliM_1$-sfGFP, CheA-mCherry, Alexa-Fluor 488). Arrows mark fluorescent clusters. The scale bar equals 5 μm.

observed to accumulate at the division plane where it co-localized with the fluorescently labeled cell division protein ZapA-sfGFP (Fig. 5B). Time-lapse microscopy and quantification of the fluorescent foci's fluorescence intensity (Fig. 6A and B) strongly suggested that targeting of *Sp*HubP to the cell division plane resulted in formation of the minor *Sp*HubP cluster that is observed at the new, nonflagellated cell poles after completion of cell division and fission. The fluorescent signal at the new cell pole rapidly gained intensity (almost reaching fluorescent intensity observed in the division plane within 10 min; Fig. 6B), strongly indicating an immediate recruitment of further copies of *Sp*HubP to the new cell pole. The signal further increased significantly during cell growth over 40 min (corresponding to one generation time) until reaching the intensity observed at the opposite pole. Both major and minor *Sp*HubP clusters displayed fluorescence recovery after complete bleaching with a half-time of about 3.2 min (major cluster) and 3.7 min (minor cluster). Thus, at least a fraction of *Sp*HubP proteins within the clusters is constantly exchanged, or further copies of the protein are constantly recruited to both clusters (Fig. 5D).

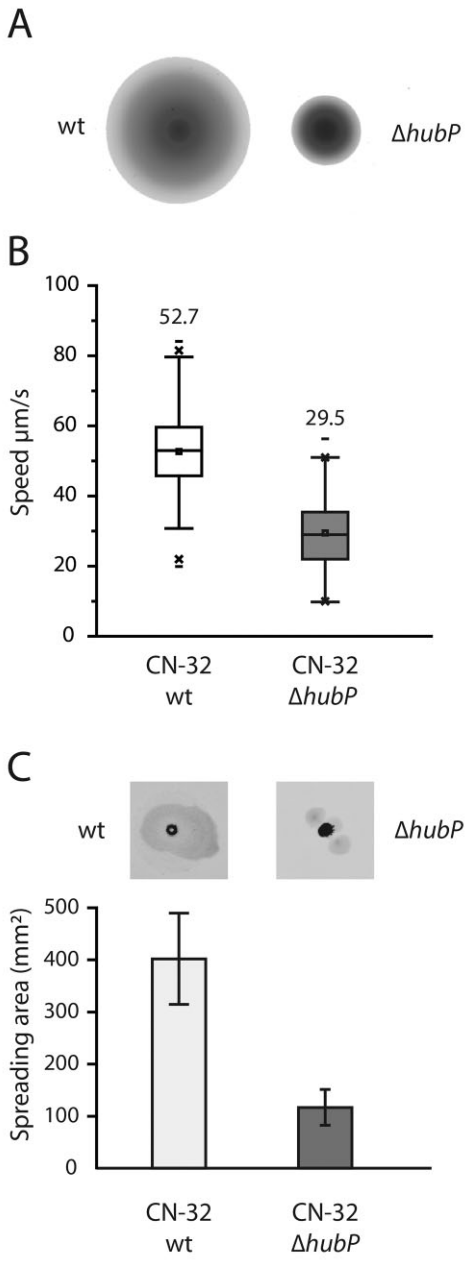

Fig. 4. *Sp*HubP is required for normal motility in *S. putrefaciens* CN-32.
A. Contribution of *Sp*HubP to spreading in soft agar. There was 3 µl of exponentially growing cultures of the corresponding strains placed on an agar plate solidified with 0.25 % agar and incubated for 16 h.
B. Contribution of *Sp*HubP to flagellar performance. Displayed is the swimming speed of wild-type and *ΔhubP* strains. The box represents the interquartile range of the data. The average and the median are shown as '□' and '—', and the whiskers denote the data range of the 5th and 95th percentile. Minimum and maximum are represented by 'x'. Swimming speed was determined for 200 cells each. Performance of the wild-type flagellar motor is significantly different from that of *ΔhubP*-mutant cells (ANOVA, *P* value 0.05).
C. Contribution of *Sp*HubP to twitching motility. The micrographs show images of the radial extension formed by twitching cells, the quantification of which is displayed below. The error bars show the standard deviation of five independent experiments.

The same localization pattern for *Sp*HubP occurred in *S. putrefaciens* cells in which the full gene locus encoding the primary polar flagellar system including *flhF* was deleted (ΔclusterI) (Fig. S9B), confirming that neither FlhF nor any other component of the polar flagellum is directly or indirectly required to target *Sp*HubP to the cell pole or division plane. When expressing a truncated version of *hubP* which only encodes the N-terminal part including the signal sequence and the predicted peptidoglycan-binding LysM domain (aa 1–134), we observed a localization pattern reminiscent to that of full-length *Sp*HubP-sfGFP (Fig. 5C). We thus concluded that the N-terminal LysM-containing domain of *Sp*HubP is sufficient for specific cellular targeting of the protein. When full-length *Sp*HubP-sfGFP or LysM-mCherry was heterologously produced in *E. coli*, both proteins similarly localized to the cell pole regions, the cell envelope, and the division plane (Figs S5 and S9C). Thus, the LysM-targeted localization of *Sp*HubP is not specific for *Shewanella*. Notably, ectopic overproduction of *Sp*HubP-sfGFP in *S. putrefaciens* CN-32 did not result in polar enrichment of the protein, but the excessive amounts were rather targeted to and accumulated at the cell envelope and division plane. These cells exhibited a distinct phenotype during growth in planktonic cultures, i.e. the occurrence of numerous smaller and elongated cells as well as chains of cells that had not separated after completion of cell division. This finding is indicating that an excess of *Sp*HubP interferes with normal cell division (Fig. S9B and D). Because a similar phenotype was observed upon overproduction of LysM-sfGFP, the effect is likely conferred by the N-terminal periplasmic domain of *Sp*HubP.

Sp*HubP, but not FlhF, targets the* oriC *to the cell pole during cell division*

*Vc*HubP has been shown to orchestrate polar localization of the *oriCI* of the larger of the two *V. cholerae* chromosomes. To determine whether or not *Sp*HubP fulfills a similar function in *S. putrefaciens* CN-32, we fused the ParB (Sputcn32_3965) C-terminus to mCherry. The hybrid gene was chromosomally integrated to replace the native *parB*. ParB is an origin-associated centromere-binding protein and thus marks the localization of the chromosomal origin. We observed no phenotype with respect to cell morphology or growth rate in the resulting strain (*mCherry-parB*), indicating that the fusion protein is fully functional.

The mCherry-ParB fusion enabled us to follow chromosome segregation in CN-32 over the cell cycle by fluorescence microscopy (Fig. 6A). Under the growth conditions

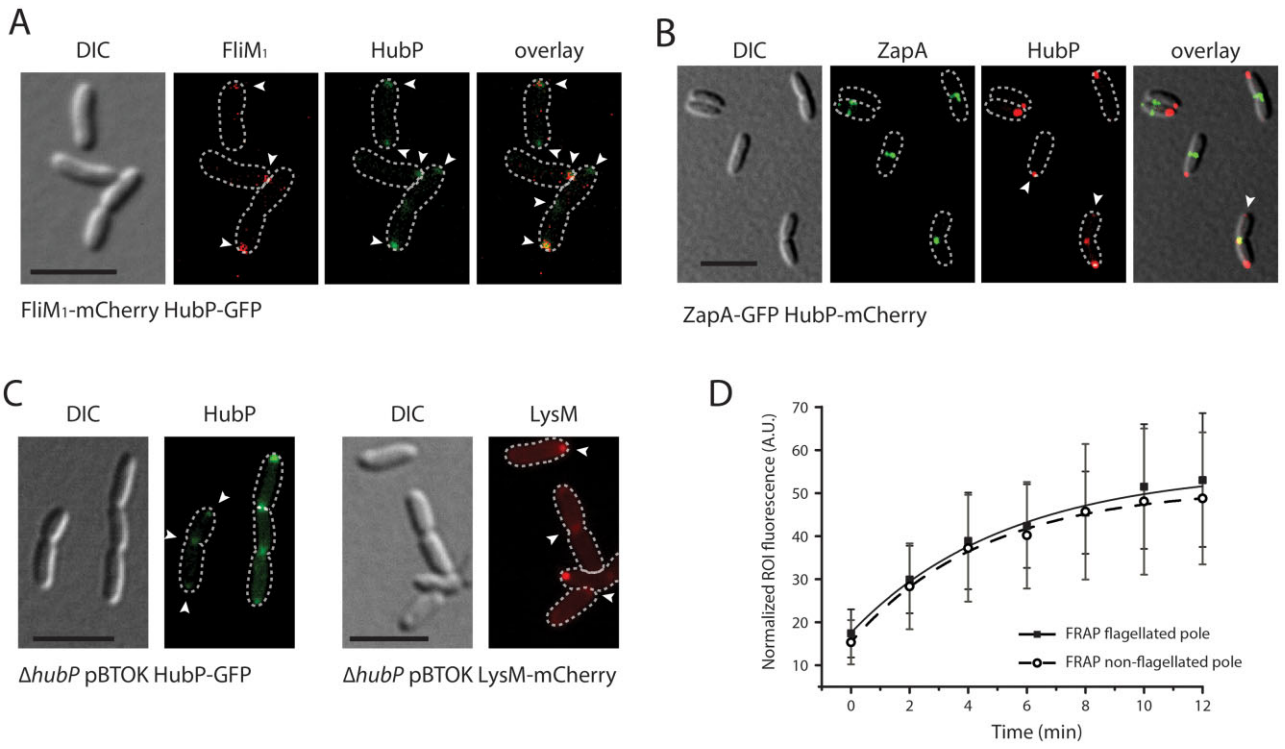

Fig. 5. Localization patterns of *Sp*HubP. Displayed are DIC and fluorescent micrographs of cells harboring fluorescently labeled components as indicated below the corresponding panels. Arrows indicate the position of fluorescent clusters. The scale bar equals 5 μm.
A. *Sp*HubP-sfGFP co-localizes with FliM$_1$ at the corresponding poles but also forms a minor cluster at the opposite cell pole.
B. *Sp*HubP-mCherry also accumulates at the division plane where it co-localizes with ZapA-sfGFP.
C. Localization pattern of *Sp*HubP-sfGFP (left panels) and its periplasmic domain (LysM-mCherry; right panels) upon ectopic production.
D. Rate of *Sp*HubP exchange as determined by FRAP. Displayed is the normalized averaged fluorescence intensity as a function of time for *Sp*HubP-sfGFP at the flagellated (black squares) and the non-flagellated (white circles) pole. Error bars display the standard error. The poles were defined prior to bleaching by co-localization with FliM$_1$-mCherry.

applied, a new replication was already initiated before cell separation, resulting in cells with four mCherry-ParB foci (33% of the population). In wild-type cells, mCherry-ParB fluorescent foci moved towards the opposite cell pole until they co-localized with fluorescently tagged *Sp*HubP directly at the cell pole. In contrast, when *Sp*HubP was absent, the mCherry-ParB foci remained at 1/4 or 3/4 position of the cell and did not resume full localization to the cell pole (Fig. 6C and D, Fig. S10A and B). Based on these observations, we concluded that *Sp*HubP has a function in chromosome segregation and is required for recruitment of *oriC* to the cell pole. Notably, the difference in chromosome segregation between wild-type and *ΔhubP* cells did not result in a significant phenotype with respect to growth or cell morphology. However, we noticed a slight difference in the timing of cell division: Under our experimental conditions, wild-type cells consistently exhibited a visible constriction when cells reached a length of 4.5 μm. In contrast, in *ΔhubP*-mutant cells, formation of the constriction occurred at less-defined cell lengths in a range of 3.6–4.4 μm. In contrast, polar localization of mCherry-ParB-marked *oriC* was unaffected by the presence or absence of FlhF (Fig. S10B).

Taken together, we have shown here that *S. putrefaciens* CN-32 possesses two distinct polar landmark systems, FlhF and *Sp*HubP. Both proteins display distinct localization patterns, and while FlhF regulates the number and polarity of the primary flagellar system, *Sp*HubP is required to target the chromosomal origin region and the chemotaxis system to the designated cell pole and likely performs some additional functions with respect to cellular motility (Fig. S11).

Discussion

For the vast majority of bacterial species, proper spatiotemporal regulation of cell polarity is crucial for a number of important or even essential cellular processes, such as chromosome segregation and cell division, differentiation, and cell motility (Treuner-Lange and Søgaard-Andersen, 2014). The latter is particularly evident for polarly flagellated bacterial species. These bacteria need to synthesize one or more new flagellar machineries at the designated cell pole, and this process often has to be strictly coordinated with the cell cycle to ensure that the daughter cell is immediately motile after separation from the mother cell

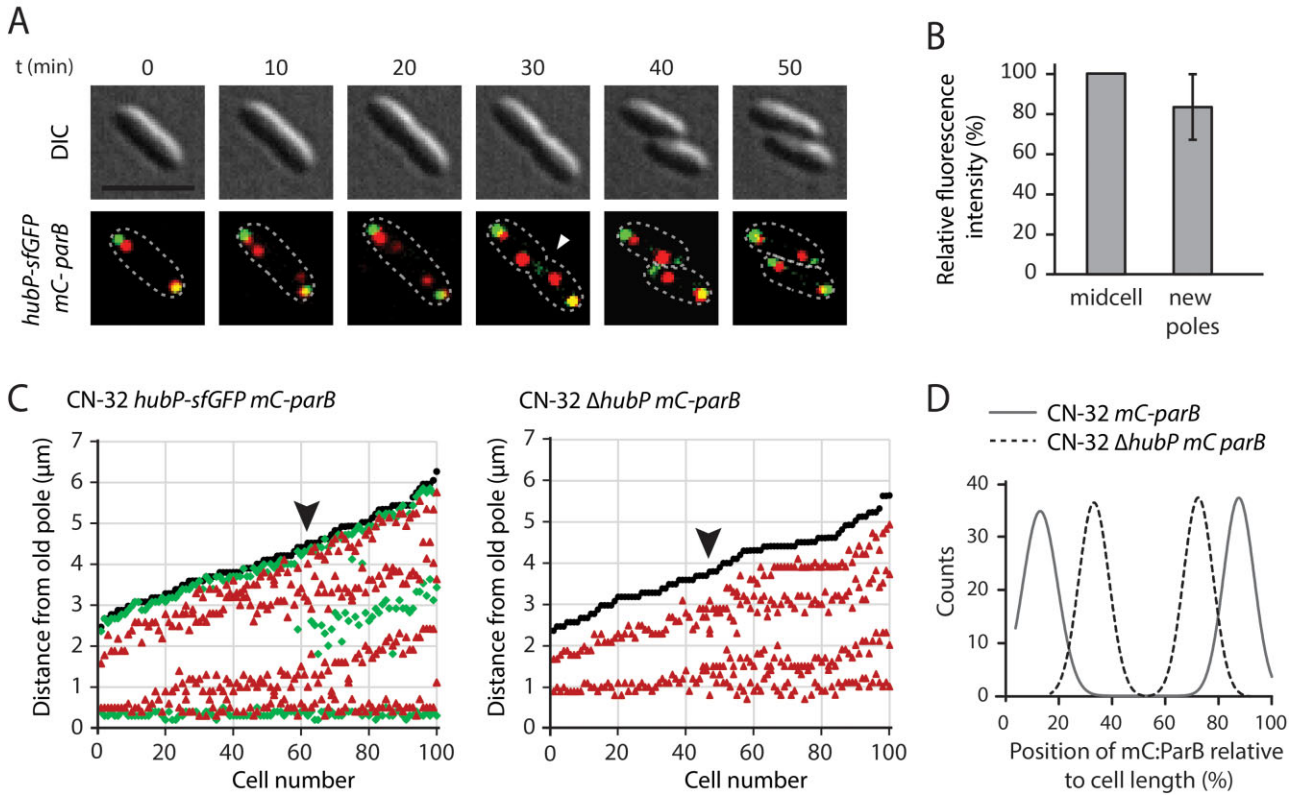

Fig. 6. Localization of *oriC* in dependence of *Sp*HubP.
A. Localization patterns of *Sp*HubP-sfGFP and ParB-mCherry during a full cell cycle. Shown are DIC (upper panel) and corresponding fluorescent micrographs (lower panel) of cells in which ParB as a marker for *oriC* was labeled with mCherry and *Sp*HubP was labeled with sfGFP. Yellow spots mark areas in which ParB and *Sp*HubP co-localize. The scale bar represents 5 µm.
B. HubP-sfGFP fluorescence intensity at midcell prior to cell fission and at each new cell pole 5–10 min after cell fission.
C. Left panel: Positioning of *Sp*HubP-sfGFP (green) and mCherry-ParB (*mC-parB*; red) relative to the cell length (black line). Right panel: Positioning of mCherry-ParB (*mC-parB*; red) relative to the cell length (black line) in the absence of *Sp*HubP. A corresponding image also displaying fluorescence intensity can be found in Fig. S10A.
D. Line scan analysis of the average mCherry-ParB (*mC-parB*) fluorescence intensity relative to the cell length. In wild-type cells (solid line) the *oriC* is localized close to the cell poles while it remains at a 1/3 position in *ΔhubP* cells (dashed line).

(Chilcott and Hughes, 2000; Ryan and Shapiro, 2003). In most bacterial species, motor functions can be modulated by one or more associated chemotaxis systems which allow biased movement towards a source of attractant or away from a repellent (Porter *et al.*, 2011; Sourjik and Wingreen, 2012). Components of bacterial chemotaxis systems are commonly arranged in large macromolecular clusters whose size has allowed their visualization and structural characterization by means of electron cryo tomography (Zhang *et al.*, 2007; Briegel *et al.*, 2009; 2012; Liu *et al.*, 2012). In a number of bipolarly or unisemipolarly flagellated bacterial species, such as *Caulobacter crescentus*, *P. aeruginosa* and *V. cholerae*, specific chemotaxis arrays localize in discrete foci at or close to the flagellated cell pole (Alley *et al.*, 1992; Wadhams *et al.*, 2003; Bardy and Maddock, 2005; Ringgaard *et al.*, 2011). This proximity of the chemotaxis system and the receiving flagellar motors has been suggested to facilitate rapid signal exchange via CheY and, hence, chemotactic efficiency (Sourjik and Berg, 2002; Lipkow *et al.*, 2005; Ringgaard *et al.*, 2014), and to ensure the inheritance of a functional chemotaxis array upon division (Jones and Armitage, 2015). *S. putrefaciens* CN-32 belongs to the bacterial species which are equipped with two complete distinct flagellar systems, a primary polar and a secondary lateral system. Under appropriate conditions, both systems are synchronously assembled (Bubendorfer *et al.*, 2012). Our study demonstrates that also in *Shewanella*, the chemotaxis cluster is localized to the flagellated cell pole. We have previously shown that the polar flagellar system primarily mediates cellular propulsion and is directly addressed by CheY. In contrast, the secondary system constantly rotates in a counterclockwise direction and does not respond to the chemotaxis system. This is likely due to the absence of the conserved N-terminal CheY-binding motif in the $FliM_2$ motor protein of the secondary system (Bubendorfer *et al.*, 2014). Thus, in *S. putrefaciens* CN-32, the primary flagellar motor and its

corresponding chemotaxis system are localized in close proximity, which likely enables rapid signal exchange via phosphorylated CheY. In contrast, the lateral filaments operate independently to curb the cellular turning angles during chemotaxis to increase spreading efficiency of the population (Bubendorfer *et al*., 2014).

The close proximity of chemotaxis and flagellar systems in various bacterial species might lead to the speculation that polar localization of both molecular machines is mediated by the same polar landmark system. Correspondingly, previous studies on *P. aeruginosa* strongly indicated that both the polar flagellar system as well as at least one of the chemotaxis arrays depend on the polar targeting system FlhF/FlhG (Kulasekara *et al*., 2013). In contrast, in *V. cholerae*, polar localization of the chemotaxis cluster is independent of FlhF (Ringgaard *et al*., 2011) but instead requires the multidomain protein HubP (Yamaichi *et al*., 2012). Our studies demonstrate that in *S. putrefaciens* CN-32, the GTPase FlhF specifically serves as the landmark protein for polar localization of the flagellar system and exhibits the corresponding localization to the old cell pole. In *S. putrefaciens* CN-32, deletion of *flhF* negatively affects production of flagella and results in displacement of the flagellum from the cell pole to more lateral positions. These data are fully consistent with those obtained for other polarly flagellated gammaproteobacteria (summarized in Kazmierczak and Hendrixson, 2013). In contrast to the primary flagellar system, normal polar localization of the chemotaxis system in *S. putrefaciens* CN-32 occurs independently of FlhF and requires the presence of another polar multidomain landmark protein, which we identified as the functional ortholog of *Vc*HubP.

Along most of their length, *Vc*HubP and *Sp*HubP exhibit little similarity at the amino acid level with the exception of the N-terminal and far C-terminal sections (Figs S6, S7, S11). The conserved N-terminal section harbors the periplasmic part of HubP including the LysM domain and the downstream transmembrane domain. In both species, this LysM-containing part of the protein appears to be required for targeting HubP to the designated cellular compartment. The localization pattern of *Sp*HubP is complex: In most cells, the protein forms a distinct cluster at the flagellated cell pole and a smaller cluster at the opposite pole. As indicated by FRAP experiments, *Sp*HubP molecules in both major and minor clusters are constantly exchanged at a similar rate. During cell division, the minor *Sp*HubP cluster appears to increase in size while the chromosomal origin is moved towards that pole. Overproduction of both full-length *Sp*HubP-sfGFP and LysM-sfGFP did not lead to infinite growth of the polar clusters, indicating that only a certain amount of *Sp*HubP may join these clusters. Excess *Sp*HubP occurring in the cell envelope may then be targeted to the cellular division plane. After completion of division, the new poles of both mother and daughter cells bear the minor *Sp*HubP cluster while the major cluster remains at the old pole which is decorated with the primary flagellar and the corresponding chemotaxis system. Thus, similar to what has been shown for TipN in *C. crescentus*, this minor *Sp*HubP cluster might serve as a marker for future polar assembly sites in the progeny cells (Huitema *et al*., 2006; Lam *et al*., 2006). Overproduction of TipN in *C. crescentus* results in the formation of lateral cell poles and leads to cellular branching. In contrast, in *S. putrefaciens* CN-32, *Sp*HubP-sfGFP and LysM-sfGFP do not form subpolar clusters upon overproduction but diffusively accumulate in the cell envelope and at the cell division plane. We thus hypothesize that the observed phenotype with respect to cell size and cell separation in *S. putrefaciens* CN-32 at excessive levels of *Sp*HubP (or its periplasmic part) might rather be due to interference between cell division proteins and the periplasmic domain of *Sp*HubP. The homologous periplasmic region of *P. aeruginosa* FimV has previously been shown to bind peptidoglycan (Wehbi *et al*., 2011) and, upon overproduction, may lead to cell elongation, vaguely reminiscent of the phenotype observed in CN-32 (Semmler *et al*., 2000). It remains to be shown how *Vc*HubP, *Sp*HubP or FimV are targeted to the cell pole and/or the division site. It might be speculated that this targeting is due to specific regions within the peptidoglycan, such as the nascent cell wall formed during cell fission, and that the resulting minor cluster of HubP is then required to recruit further HubP copies to the new cell pole after cell separation. When *Sp*HubP-sfGFP or LysM-sfGFP are ectopically produced in *E. coli*, the protein localizes to the cell poles and cell division plane as observed in *Shewanella*, suggesting that similar structures are recognized by the periplasmic region of *Sp*HubP in both species. However, it should be noted that *Vc*HubP is directed to the cell envelope in *E. coli*, but does not exhibit its normal localization pattern in this species.

In contrast to the periplasmic region, the cytoplasmic parts of *Sp*HubP and *Vc*HubP are far less conserved and, in addition, this section is considerably shorter in *Sp*HubP (Figs S6 and S7). However, both proteins harbor within this domain 9 or 10 copies of an imperfect repeat of an amino acid motif that is highly enriched in aspartate and glutamate residues and thus imparts a highly acidic character on the protein. Studies on *Vc*HubP have provided evidence that the protein exerts its function as a polar hub by directing ParA-like ATPases, which are commonly implicated in spatiotemporal organization processes in bacteria (Lutkenhaus, 2012), to the designated cell pole (Yamaichi *et al*., 2012). ParA1, required for segregation of the larger of the two *V. cholerae* chromosomes, has been shown to directly interact with the repeat region of *Vc*HubP and this might be similarly true for *Sp*ParA and *Sp*HubP, because a deletion in *hubP* results in a very similar phenotype with respect to chromosome segregation in both *V. cholerae*

and *S. putrefaciens*. Direct interaction of *Vc*ParC, which is implicated in positioning of the chemotaxis machinery (Ringgaard *et al*., 2011), and *Vc*HubP could not be demonstrated, strongly indicating that not all *Vc*HubP client proteins have been identified yet (Yamaichi *et al*., 2012). Accordingly, deletion of the obvious *Vc*ParC ortholog in *S. putrefaciens* CN-32 (Sputcn32_2553) did not exhibit a major phenotype with respect to chemotactic swimming (data not shown). The findings strongly suggest that other, yet unidentified, factors are required to mediate polar recruitment of the chemotaxis complex by HubP.

In *S. putrefaciens*, polar targeting of FlhF and *Sp*HubP and localization of flagellar and chemotaxis systems appear to occur independently. However, when *Sp*HubP is absent, FlhF and, accordingly, $FliM_1$ was observed at the cell pole in a significantly smaller cell population, indicating that *Sp*HubP might be involved in regulating the ability of FlhF to accumulate at the cell pole and to recruit basal body proteins. A previous study has provided evidence that a high amount of FlhG negatively affects polar localization of FlhF in *V. alginolyticus* (Kusumoto *et al*., 2008). Recent work on the same species provided further conclusive evidence that polar localization of FlhG strongly depends on the ATPase activity of the protein and has a strong effect on the polar accumulation of FlhF and, hence, the formation of flagella at the cell pole (Ono *et al*., 2015). Notably, HubP was shown to directly interact with FlhF and FlhG in *V. cholerae* (Yamaichi *et al*., 2012), and we have shown here that also in *S. putrefaciens* CN-32, FlhG localizes to the flagellated cell pole in a *Sp*HubP-dependent fashion. This may suggest that while *Sp*HubP might not directly localize FlhF, it might mediate proper FlhF-FlhG interactions at the cell pole to restrict the formation of the number of polar flagella to one in the appropriate number of cells. In addition, we could provide evidence that *Sp*FlhF and *Sp*FlhG interact *in vitro* and that the N-terminal section of *Sp*FlhG stimulates the GTPase activity of *Sp*FlhF. Thus, *Sp*HubP-mediated interaction between FlhF and FlhG and control of the GTPase activity might affect FlhF-related functions such as polar accumulation and recruitment of flagellar components, but also flagellar performance, as has recently been suggested for *P. aeruginosa* (Schniederberend *et al*., 2013). Accordingly, a deletion of *hubP* in both *V. cholerae* and *S. putrefaciens* CN-32 resulted in a significantly decreased ability to navigate through soft agar. In *V. cholerae*, this phenotype has been mainly attributed to a decrease in the chemotactic drift of the population due to the, on average, increased distance between the chemotaxis machinery and the flagellar motor, resulting in a limited ability to induce directional switches appropriately (Ringgaard *et al*., 2011; Yamaichi *et al*., 2012). However, we additionally found that in *S. putrefaciens* CN-32 *ΔhubP* mutants, the average swimming speed in planktonic cultures was significantly reduced which cannot be solely attributed to the loss of chemotaxis (Bubendorfer *et al*., 2014). While this observed decrease in swimming speed might be due to *Sp*HubP-FlhF/FlhG interaction as elaborated above, it might similarly be speculated that *Sp*HubP directly or indirectly recruits other proteins that affect flagellar functions (Boehm *et al*., 2010; Fang and Gomelsky, 2010; Paul *et al*., 2010; Kulasekara *et al*., 2013). We have shown that also type IV pili-mediated twitching motility, which requires polar assembly and disassembly of pili fibers (Burrows, 2012), is affected in *S. putrefaciens ΔhubP*. We thus expect that further interaction partners, or 'client' proteins, of *Sp*HubP remain to be identified which do not belong to the group of ParA-like proteins.

Potential HubP or FimV orthologs can be identified in a number of different bacterial genera (Semmler *et al*., 2000; Yamaichi *et al*., 2012). All of these proteins share an N-terminal periplasmic domain comprising the, putatively peptidoglycan-binding, LysM-domain. This N-terminal domain might also be involved in mediating protein–protein interactions within the periplasm or membrane (Wehbi *et al*., 2011). In addition, all these proteins are characterized by a highly acidic cytoplasmic part which appears to function as the docking region for other appropriate interaction partners. This cytoplasmic region is little conserved at the amino acid level but also with respect to protein length and the presence and organization of repeat units, and even within a group of closely related species, such as in various *Shewanella* sp., the cytoplasmic part of HubP/FimV exhibits a high degree of variation. It might thus be speculated that polar targeting within the cell by the LysM domain is conserved throughout the species. In contrast, the cytoplasmic and also the periplasmic parts may have adapted to the specific requirement of the host species for polar localization of client proteins or protein complexes. These differences might be the reason why the chemotaxis system is localized by HubP in *V. cholerae* and *S. putrefaciens* CN-32, but directly or indirectly depends on FlhF in *P. aeruginosa*. Thus, HubP/FimV proteins might have numerous different functions, including various aspects of motility and chromosome segregation as shown for *P. aeruginosa*, *V. cholerae* and *S. putrefaciens* CN-32 (Semmler *et al*., 2000; Wehbi *et al*., 2011; Yamaichi *et al*., 2012; Fig. S11). We expect that future studies on different species will identify further processes which are spatiotemporally organized by HubP/FimV proteins.

Experimental procedures

Strains, growth conditions and media

All strains used in this study are listed in Table S1. *E. coli* strains were routinely cultured in LB medium at 37°C if not indicated otherwise. *S. putrefaciens* CN-32 strains were cultivated in LB or LM (10 mM HEPES, pH 7.5; 200 mM NaCl;

0.02% yeast extract; 0.01% peptone; 15 mM lactate) media at 30°C. When required, media were supplemented with 50 μg ml^{-1} kanamycin or 10% (w/v) sucrose. Cultures of the *E. coli* conjugation strain were supplemented with 2,6-diamino-pimelic acid (DAP) to a final concentration of 300 μM. Solid media were made by an addition of 1.5% (w/v) agar. Soft agar plates for swimming assays were prepared with LB medium solidified with 0.25% (w/v) agar.

Strain constructions

General DNA manipulations were carried out according to standard protocols (Sambrook *et al*., 1989) using appropriate kits (VWR International GmbH, Darmstadt, Germany) and enzymes (Fermentas, St Leon-Rot, Germany). All vectors/plasmids used in this study are summarized in Table S2. Plasmids were delivered to *S. putrefaciens* CN-32 by conjugation from *E. coli* WM3064. Markerless in-frame deletions were generated by sequential homologous crossover using vector pNTPS-138-R6K essentially as described previously (Lassak *et al*., 2010). Vectors were constructed either by common restriction/ligation approaches using appropriate restriction enzymes, or by enzymatic assembly as previously reported (Gibson *et al*., 2009). The corresponding oligonucleotides used for cloning are listed in Table S3. To complement in-frame deletion mutants, the mutated locus was exchanged with the wild-type gene using the same sequential crossover approach. To generate fluorescent fusions, target proteins were either C- or N-terminally tagged with sfGFP, mCherry, Venus or eCFP using a flexible linker of either 6xGly, 2x(Gly-Gly-Ser), 3x(Gly-Gly-Ser) or (Gly-Ser) (for ectopic overproduction of FlhF-sfGFP and C-terminal tagging of FlhG). The nature of each fluorescent fusion is specified in detail in Table S1. All genetic fusions except those for the MCPs and for ectopic (over-)production were introduced into the chromosome to replace the native copy of the gene essentially as previously described (Bubendorfer *et al*., 2012) by markerless sequential crossover using pNTPS-138-R6K as delivery vector. The fusion to MCP0796 was established by cloning an appropriate PCR-derived DNA fragment of about 500 bp encoding the C-terminal region of the proteins into vector pJP5603-gfp (Koerdt *et al*., 2009) followed by conjugation and single homologous integration, yielding a chromosomal fusion expressed under its native promoter. Correct insertions or deletions were verified by polymerase chain reaction (PCR). Production levels and stability of fusion proteins were checked by immunofluorescence approaches and appropriate phenotypic analysis (Fig. S1). To enable coupling of maleimide-ligated Alexa dyes to the flagellar filaments, a threonine-to-cysteine (T159C) were introduced in both $FlaA_1$ and $FlaB_1$ flagellins by exchange of the appropriate codons within the corresponding genes on the chromosome, resulting in strain $FlaAB_1$-Cys. Accordingly, variants of $FlaA_2$ (T159C; T160C) and $FlaB_2$ (T156C; T159C) were constructed for specific labeling of secondary flagella. For overproduction of FlhF and FlhG and derivatives, the corresponding genes (Sputcn32_2561, *flhF*; Sputcn32_2560, *flhG*) were amplified from *S. putrefaciens* CN-32 genomic DNA by PCR using appropriate primer pairs (Table S3). The forward primer encoded a hexa-histidine tag in frame with the DNA sequence of *flhF* or *flhG*. The resultant PCR fragments were cloned into pET24d(+) (Novagen) or pGAT3 (Peränen *et al*., 1996) vectors via the introduced restriction sites. Due to enhanced purification properties of the produced protein, a truncated version of *flhF* lacking the first 10 codons of the 5′-end was overexpressed.

Overproduction of Sp*HubP-sfGFP and LysM-mCherry*

The vector pBTOK was derived by assembly of the anhydrotetracycline-inducible promoter region of pASK-IBA3plus (IBA GmbH, Göttingen, Germany) followed by the *E. coli rrnB1* T_1 and lambda phage T_0 terminator set into pBBR1-MCS5 (Kovach *et al*., 1995). The vector backbone fragment was amplified with primer pair SH501/SH502 using pBBR1-MCS5 as a template; the promoter region including the MCS of pAS-IBA3plus was derived using SH503/SH504; and the terminator region was produced using SH505/SH506 and pUC18-mini-Tn*7*T-Gm-lux (Choi *et al*., 2005) as a template. Fragment assembly was carried as previously described (Gibson *et al*., 2009). Sequence and vector map are available upon request. The sequence of *hubP-sfgfp*, the LysM domain [*Sp*HubP_AA1-134 (Sputcn32_2442_nt1-402)] and mCherry were amplified with the corresponding primer pairs. The LysM-encoding gene region and *mCherry* were joined by an overlap PCR. The resulting inserts were processed with XbaI and PspOMI and ligated into the vector. The resulting plasmid was transferred into CN-32 *ΔhubP* via conjugation. Prior to overproduction, CN-32 pBTOK-HubP-sfGFP and CN-32 pBTOK-LysM-mCherry were cultured in LB media to an OD_{600} of ~ 0.3 followed by induction with 20 ng·ml^{-1} anhydrotetracycline for 45 min.

Flagellar and hook staining

Fluorescent staining of flagellar filaments (CN-32 $FlaAB_1$-Cys) or hook structures ($FlgE_2$-Cys; Schuhmacher *et al*., 2015b) was essentially carried out on exponentially growing cells as previously described (Guttenplan *et al*., 2013) using Alexa Fluor 488 maleimide (Molecular Probes, Life Technologies) prior to microscopy.

Fluorescence microscopy

Prior to microscopy, strains were cultivated overnight in LM media and subcultured in LM until reaching exponential growth phase (OD_{600} of ~ 0.2). There was 3 μl of culture spotted on an agarose pad (LM media solidified by 1% (w/v) agarose). Fluorescence images were recorded by a Leica DMI 6000 B inverse microscope (Leica, Wetzlar, Germany) equipped with an sCMOS camera and a HCX PL APO 100×/1.4 objective using the VisiView software (Visitron Systems, Puchheim, Germany). Images were further processed using ImageJ and Adobe Illustrator CS6.

Fluorescence recovery after photobleaching (FRAP)

FRAP analyses were carried out with a Axio Imager.M1 microscope (Zeiss), a Zeiss Plan Apochromat 100×/1.40 Oil DIC (Differential Interference Contrast) objective and a

Cascade:1K CCD camera (Photometrics) equipped with a 488 nm-solid state laser and a 2D-VisiFRAP Galvo System multi-point FRAP module (Visitron Systems, Germany). Cells were cultured and immobilized on agarose pads as described above. After acquisition of a pre-bleach image, a single laser pulse of 30 ms was used to bleach individual *Sp*HubP-sfGFP clusters. Fluorescence recovery was subsequently monitored at 2-min intervals for 12 min. The integrated fluorescence intensities of the whole cell, the bleached region and an equally sized unbleached region were measured for each time point using ImageJ. After background correction, the fluorescence intensities of the bleached and unbleached regions were divided by the whole cell intensity to correct for general photobleaching during the imaging process. Average values of 10–13 cells were plotted using OriginPro 9.1. Recovery rates were determined by fitting the data obtained for the bleached region to the single exponential function F(t) = F0*exp(-x/t1) + A, where F(t) is the fluorescence at time t, A the maximum intensity, x the time in min, 1/t1 the rate constant in min^{-1} and F0 the relative fluorescence intensity at t = 0 min. In all cases, fits with R2 ≥ 0.99 were obtained. Recovery half-times were calculated according to the equation $t_{1/2} = ln(2)*t1$.

Determination of swimming speed

Cells of *S. putrefaciens* CN-32 and *S. putrefaciens* CN-32 Δ*hubP* from overnight cultures were used to inoculate LM medium to an OD_{600} of 0.02 and cultivated for 3–4 h to an OD_{600} of ~ 0.2. An aliquot of each culture was placed under a coverslip fixed by four droplets of silicone to create a space of 1–2 mm width. Movies of 12 s (157 frames) were taken with an inverse microscope (for specification, see above). Speeds of 200 cells per strain were determined using the MTrackJ plugin of ImageJ. The resulting data were tested for significance by using ANOVA ($P = 0.05$) in R version 3.0.1. Motility was further assessed by placing 3 µl of a planktonic culture of the corresponding strains on soft agar plates containing LB medium with an agar concentration of 0.25% (w/v). Plates were incubated for 12h at 30°C or overnight at room temperature. Strains to be directly compared were always placed on the same plate.

Analysis of twitching motility

Type IV pili-mediated twitching motility was assayed as described previously (Semmler *et al.*, 1999) using 1.0 % LB-agar plates at 30°C for up to 48 h.

Protein production and purification

E. coli BL21(DE3) (New England BioLabs, Frankfurt, Germany) cells carrying the appropriate expression plasmid were grown in LB medium supplemented with kanamycin (100 µg ml^{-1}) and D(+)-lactose-monohydrate (12.5 g l^{-1}) for 16 h at 30°C under rigorous shaking (150 r.p.m.). Cells were harvested (3500×*g*, 20 min, 4°C) and resuspended in lysis buffer (20 mM HEPES, pH 8.0; 250 mM NaCl; 40 mM imidazole; 20 mM $MgCl_2$ and 20 mM KCl). Cells were lysed with the M-110L Microfluidizer (Microfluidics). After centrifugation (47 850×*g*, 20 min, 4°C), the clear supernatant was loaded on a 1 ml HisTrap column (GE Healthcare) equilibrated with 10 column volumes (CV) of lysis buffer. After washing with 10 CV lysis buffer, the protein was eluted with 15 ml elution buffer (lysis buffer containing 500 mM imidazole). The protein was concentrated to ≈ 15 mg ml^{-1} using an Amicon Ultracel-10K (Millipore). The concentrated sample was applied to size-exclusion chromatography (HiLoad 26/600 Superdex 200 pg, GE Healthcare) equilibrated with SEC-buffer (20 mM HEPES, pH 7.5, 200 mM NaCl 20 mM MgCl2 and 20 mM KCl). Protein concentration was determined by a spectrophotometer (NanoDrop Lite, Thermo Scientific).

GTPase activity of FlhF

GTPase activity of FlhF was monitored by HPLC. There was 100 µM of each protein (FlhF, FlhG and/or corresponding derivatives as indicated) incubated together with 1 mM GTP in SEC-buffer for 30 min at 37°C. Reactions were stopped by flash-freezing with liquid nitrogen and stored at –20°C until measurement. HPLC measurements were performed with an Agilent 1100 Series HPLC system (Agilent Technologies, Santa Clara) and a C18 column (EC 250/4.6 Nucleodur HTec 3 µm; Macherey-Nagel, Düren, Germany). GDP and GTP were eluted with a buffer containing 50 mM KH_2PO_4, 50 mM K_2HPO_4, 10 mM tetrapentylammonium bromide and 15% (v/v) acetonitrile at 0.8 ml min^{-1} flow rate and detected at a wavelength of 253 nm in agreement with standards. GDP originating from non-enzymatic hydrolysis of GTP was determined by triplicate measurement of 1 mM GTP treated similar as the enzymatic reactions and subtracted from the quantified GDP.

Immunoblot (Western blot) analysis

Production and stability of the fusions were determined by immunoblot analyses. Protein lysates were prepared from exponentially growing cultures. Cell suspensions were uniformly adjusted to an OD_{600} of 10. Protein separation and immunoblot detection were essentially carried out as described earlier (Bubendorfer *et al.*, 2012; Binnenkade *et al.*, 2014) using polyclonal antibodies raised against mCherry, GFP (Eurogentec Deutschland GmbH, Köln, Germany) or FlhG (Schuhmacher *et al.*, 2015b). Signals were detected using the SuperSignal® West Pico Chemiluminescent Substrate (Thermo Scientific, Schwerte, Germany) and documented using a FUSION-SL chemiluminescence imager (Peqlab, Erlangen, Germany).

Acknowledgements

This project was supported by grants from the Deutsche Forschungsgemeinschaft (DFG) to KMT (TH831/5-1) in the framework of the priority program SPP1617. FR and SB were supported by the International Max Planck Research School. The project was further supported by the LOEWE excellence initiative of the state of Hesse (to GB).

We are grateful to Oliver Leicht and Martin Thanbichler at the Philipps-Universität Marburg for help with the FRAP analysis and to Wieland Steinchen of the Bange lab for his assistance during HPLC measurements. We would also like

to thank Martin Thanbichler and Anke Treuner-Lange for critically reading and commenting on the manuscript.

Conflict of interest

The authors declare no conflict of interest.

References

Alley, M.R., Maddock, J.R., and Shapiro, L. (1992) Polar localization of a bacterial chemoreceptor. *Genes Dev* **6:** 825–836.

Altegoer, F., Schuhmacher, J., Pausch, P., and Bange, G. (2014) From molecular evolution to biobricks and synthetic modules: a lesson by the bacterial flagellum. *Biotechnol Genet Eng Rev* **30:** 49–64.

Balaban, M., Joslin, S.N., and Hendrixson, D.R. (2009) FlhF and its GTPase activity are required for distinct processes in flagellar gene regulation and biosynthesis in *Campylobacter jejuni*. *J Bacteriol* **191:** 6602–6611.

Bange, G., and Sinning, I. (2013) SIMIBI twins in protein targeting and localization. *Nat Struct Mol Biol* **20:** 776–780.

Bange, G., Petzold, G., Wild, K., Parlitz, R.O., and Sinning, I. (2007) The crystal structure of the third signal-recognition particle GTPase FlhF reveals a homodimer with bound GTP. *Proc Natl Acad Sci USA* **104:** 13621–13625.

Bange, G., Kümmerer, N., Grudnik, P., Lindner, R., Petzold, G., Kressler, D., *et al*. (2011) Structural basis for the molecular evolution of SRP-GTPase activation by protein. *Nat Struct Mol Biol* **18:** 1376–1380.

Bardy, S.L., and Maddock, J.R. (2005) Polar localization of a soluble methyl-accepting protein of *Pseudomonas aeruginosa*. *J Bacteriol* **187:** 7840–7844.

Binnenkade, L., Teichmann, L., and Thormann, K.M. (2014) Iron triggers lambdaSo prophage induction and release of extracellular DNA in *Shewanella oneidensis* MR-1 biofilms. *Appl Environ Microbiol* **80:** 5304–5316.

Boehm, A., Kaiser, M., Li, H., Spangler, C., Kasper, C.A., Ackermann, M., *et al*. (2010) Second messenger-mediated adjustment of bacterial swimming velocity. *Cell* **141:** 107–116.

Briegel, A., Ortega, D.R., Tocheva, E.I., Wuichet, K., Li, Z., Chen, S., *et al*. (2009) Universal architecture of bacterial chemoreceptor arrays. *Proc Natl Acad Sci USA* **106:** 17181–17186.

Briegel, A., Li, X., Bilwes, A.M., Hughes, K.T., Jensen, G.J., and Crane, B.R. (2012) Bacterial chemoreceptor arrays are hexagonally packed trimers of receptor dimers networked by rings of kinase and coupling proteins. *Proc Natl Acad Sci USA* **109:** 3766–3771.

Bubendorfer, S., Held, S., Windel, N., Paulick, A., Klingl, A., and Thormann, K.M. (2012) Specificity of motor components in the dual flagellar system of *Shewanella putrefaciens* CN-32. *Mol Microbiol* **83:** 335–350.

Bubendorfer, S., Koltai, M., Rossmann, F., Sourjik, V., and Thormann, K.M. (2014) Secondary bacterial flagellar system improves bacterial spreading by increasing the directional persistence of swimming. *Proc Natl Acad Sci USA* **111:** 11485–11490.

Burrows, L.L. (2012) *Pseudomonas aeruginosa* twitching motility: type IV pili in action. *Annu Rev Microbiol* **66:** 493–520.

Chilcott, G.S., and Hughes, K.T. (2000) Coupling of flagellar gene expression to flagellar assembly in *Salmonella enterica* serovar *typhimurium* and *Escherichia coli*. *Microbiol Mol Biol Rev* **64:** 694–708.

Choi, K.H., Gaynor, J.B., White, K.G., Lopez, C., Bosio, C.M., Karkhoff-Schweizer, R.R., and Schweizer, H.P. (2005) A Tn*7*-based broad-range bacterial cloning and expression system. *Nat Methods* **2:** 443–448.

Correa, N.E., Peng, F., and Klose, K.E. (2005) Roles of the regulatory proteins FlhF and FlhG in the *Vibrio cholerae* flagellar transcription hierarchy. *J Bacteriol* **187:** 6324–6332.

Dasgupta, N., Arora, S.K., and Ramphal, R. (2000) fleN, a gene that regulates flagellar number in *Pseudomonas aeruginosa*. *J Bacteriol* **182:** 357–364.

Davis, N.J., Cohen, Y., Sanselicio, S., Fumeaux, C., Ozaki, S., Luciano, J., *et al*. (2013) De- and repolarization mechanism of flagellar morphogenesis during a bacterial cell cycle. *Genes Dev* **27:** 2049–2062.

Ewing, C.P., Andreishcheva, E., and Guerry, P. (2009) Functional characterization of flagellin glycosylation in *Campylobacter jejuni* 81–176. *J Bacteriol* **191:** 7086–7093.

Fang, X., and Gomelsky, M. (2010) A post-translational, c-di-GMP-dependent mechanism regulating flagellar motility. *Mol Microbiol* **76:** 1295–1305.

Gibson, D.G., Young, L., Chuang, R.Y., Venter, J.C., Hutchison, C.A., 3rd, and Smith, H.O. (2009) Enzymatic assembly of DNA molecules up to several hundred kilobases. *Nat Methods* **6:** 343–345.

Green, J.C., Kahramanoglou, C., Rahman, A., Pender, A.M., Charbonnel, N., and Fraser, G.M. (2009) Recruitment of the earliest component of the bacterial flagellum to the old cell division pole by a membrane-associated signal recognition particle family GTP-binding protein. *J Mol Biol* **391:** 679–690.

Guttenplan, S.B., Shaw, S., and Kearns, D.B. (2013) The cell biology of peritrichous flagella in *Bacillus subtilis*. *Mol Microbiol* **87:** 211–229.

Huitema, E., Pritchard, S., Matteson, D., Radhakrishnan, S.K., and Viollier, P.H. (2006) Bacterial birth scar proteins mark future flagellum assembly site. *Cell* **124:** 1025–1037.

Jones, C.W., and Armitage, J.P. (2015) Positioning of bacterial chemoreceptors. *Trends Microbiol* **23:** 247–256.

Kazmierczak, B.I., and Hendrixson, D.R. (2013) Spatial and numerical regulation of flagellar biosynthesis in polarly flagellated bacteria. *Mol Microbiol* **88:** 655–663.

Koerdt, A., Paulick, A., Mock, M., Jost, K., and Thormann, K.M. (2009) MotX and MotY are required for flagellar rotation in *Shewanella oneidensis* MR-1. *J Bacteriol* **191:** 5085–5093.

Kovach, M.E., Elzer, P.H., Hill, D.S., Robertson, G.T., Farris, M.A., Roop, R.M., 2nd, and Peterson, K.M. (1995) Four new derivatives of the broad-host-range cloning vector pBBR1MCS, carrying different antibiotic-resistance cassettes. *Gene* **166:** 175–176.

Kulasekara, B.R., Kamischke, C., Kulasekara, H.D., Christen, M., Wiggins, P.A., and Miller, S.I. (2013) c-di-GMP heterogeneity is generated by the chemotaxis machinery to regulate flagellar motility. *Elife* **2:** e01402.

Kusumoto, A., Kamisaka, K., Yakushi, T., Terashima, H., Shinohara, A., and Homma, M. (2006) Regulation of polar

flagellar number by the *flhF* and *flhG* genes in *Vibrio alginolyticus*. *J Biochem* **139:** 113–121.
Kusumoto, A., Shinohara, A., Terashima, H., Kojima, S., Yakushi, T., and Homma, M. (2008) Collaboration of FlhF and FlhG to regulate polar-flagella number and localization in *Vibrio alginolyticus*. *Microbiology* **154:** 1390–1399.
Laloux, G., and Jacobs-Wagner, C. (2014) How do bacteria localize proteins to the cell pole? *J Cell Sci* **127:** 11–19.
Lam, H., Schofield, W.B., and Jacobs-Wagner, C. (2006) A landmark protein essential for establishing and perpetuating the polarity of a bacterial cell. *Cell* **124:** 1011–1023.
Lassak, J., Henche, A.L., Binnenkade, L., and Thormann, K.M. (2010) ArcS, the cognate sensor kinase in an atypical Arc system of *Shewanella oneidensis* MR-1. *Appl Environ Microbiol* **76:** 3263–3274.
Lipkow, K., Andrews, S.S., and Bray, D. (2005) Simulated diffusion of phosphorylated CheY through the cytoplasm of *Escherichia coli*. *J Bacteriol* **187:** 45–53.
Liu, J., Hu, B., Morado, D.R., Jani, S., Manson, M.D., and Margolin, W. (2012) Molecular architecture of chemoreceptor arrays revealed by cryoelectron tomography of *Escherichia coli* minicells. *Proc Natl Acad Sci USA* **109:** E1481–E1488.
Lutkenhaus, J. (2012) The ParA/MinD family puts things in their place. *Trends Microbiol* **20:** 411–418.
Murray, T.S., and Kazmierczak, B.I. (2006) FlhF is required for swimming and swarming in *Pseudomonas aeruginosa*. *J Bacteriol* **188:** 6995–7004.
Obuchowski, P.L., and Jacobs-Wagner, C. (2008) PfIl, a protein involved in flagellar positioning in *Caulobacter crescentus*. *J Bacteriol* **190:** 1718–1729.
Ono, H., Takashima, A., Hirata, H., Homma, M., and Kojima, S. (2015) The MinD homolog FlhG regulates the synthesis of the single polar flagellum of *Vibrio alginolyticus*. *Mol Microbiol* **98:** 130–141. doi: 10.1111/mmi.13109
Pandza, S., Baetens, M., Park, C.H., Au, T., Keyhan, M., and Matin, A. (2000) The G-protein FlhF has a role in polar flagellar placement and general stress response induction in *Pseudomonas putida*. *Mol Microbiol* **36:** 414–423.
Paul, K., Nieto, V., Carlquist, W.C., Blair, D.F., and Harshey, R.M. (2010) The c-di-GMP binding protein YcgR controls flagellar motor direction and speed to affect chemotaxis by a 'backstop brake' mechanism. *Mol Cell* **38:** 128–139.
Peränen, J., Rikkonen, M., Hyvonen, M., and Kaariainen, L. (1996) T*7* vectors with modified T*7lac* promoter for expression of proteins in *Escherichia coli*. *Anal Biochem* **236:** 371–373.
Porter, S.L., Wadhams, G.H., and Armitage, J.P. (2011) Signal processing in complex chemotaxis pathways. *Nat Rev Microbiol* **9:** 153–165.
Reyes-Lamothe, R., Nicolas, E., and Sherratt, D.J. (2012) Chromosome replication and segregation in bacteria. *Annu Rev Genet* **46:** 121–143.
Ringgaard, S., Schirner, K., Davis, B.M., and Waldor, M.K. (2011) A family of ParA-like ATPases promotes cell pole maturation by facilitating polar localization of chemotaxis proteins. *Genes Dev* **25:** 1544–1555.
Ringgaard, S., Zepeda-Rivera, M., Wu, X., Schirner, K., Davis, B.M., and Waldor, M.K. (2014) ParP prevents dissociation of CheA from chemotactic signaling arrays and tethers them to a polar anchor. *Proc Natl Acad Sci USA* **111:** E255–E264.
Ryan, K.R., and Shapiro, L. (2003) Temporal and spatial regulation in prokaryotic cell cycle progression and development. *Annu Rev Biochem* **72:** 367–394.
Sambrook, K., Fritsch, E.F., and Maniatis, T. (1989) *Molecular Cloning: A Laboratory Manual*. Cold Spring Harbor, NY: Cold Spring Harbor Press.
Schniederberend, M., Abdurachim, K., Murray, T.S., and Kazmierczak, B.I. (2013) The GTPase activity of FlhF is dispensable for flagellar localization, but not motility, in *Pseudomonas aeruginosa*. *J Bacteriol* **195:** 1051–1060.
Schuhmacher, J.S., Thormann, K.M., and Bange, G. (2015a) How bacteria maintain location and function of flagella? *FEMS Microbiol Rev* (in press). pii: fuv034.
Schuhmacher, J.S., Rossmann, F., Dempwolff, F., Knauer, C., Altegoer, F., Steinchen, W., *et al*. (2015b) MinD-like ATPase FlhG effects location and number of bacterial flagella during C-ring assembly. *Proc Natl Acad Sci USA* **112:** 3092–3097.
Semmler, A.B., Whitchurch, C.B., and Mattick, J.S. (1999) A re-examination of twitching motility in *Pseudomonas aeruginosa*. *Microbiology* **145** (Part 10): 2863–2873.
Semmler, A.B., Whitchurch, C.B., Leech, A.J., and Mattick, J.S. (2000) Identification of a novel gene, *fimV*, involved in twitching motility in *Pseudomonas aeruginosa*. *Microbiology* **146:** 1321–1332.
Sourjik, V., and Berg, H.C. (2002) Binding of the *Escherichia coli* response regulator CheY to its target measured in vivo by fluorescence resonance energy transfer. *Proc Natl Acad Sci USA* **99:** 12669–12674.
Sourjik, V., and Wingreen, N.S. (2012) Responding to chemical gradients: bacterial chemotaxis. *Curr Opin Cell Biol* **24:** 262–268.
Thanbichler, M. (2010) Synchronization of chromosome dynamics and cell division in bacteria. *Cold Spring Harb Perspect Biol* **2:** a000331.
Treuner-Lange, A., and Søgaard-Andersen, L. (2014) Regulation of cell polarity in bacteria. *J Cell Biol* **206:** 7–17.
Wadhams, G.H., Warren, A.V., Martin, A.C., and Armitage, J.P. (2003) Targeting of two signal transduction pathways to different regions of the bacterial cell. *Mol Microbiol* **50:** 763–770.
Wehbi, H., Portillo, E., Harvey, H., Shimkoff, A.E., Scheurwater, E.M., Howell, P.L., and Burrows, L.L. (2011) The peptidoglycan-binding protein FimV promotes assembly of the *Pseudomonas aeruginosa* type IV pilus secretin. *J Bacteriol* **193:** 540–550.
Yamaichi, Y., Bruckner, R., Ringgaard, S., Möll, A., Cameron, D.E., Briegel, A., *et al*. (2012) A multidomain hub anchors the chromosome segregation and chemotactic machinery to the bacterial pole. *Genes Dev* **26:** 2348–2360.
Zhang, P., Khursigara, C.M., Hartnell, L.M., and Subramaniam, S. (2007) Direct visualization of *Escherichia coli* chemotaxis receptor arrays using cryo-electron microscopy. *Proc Natl Acad Sci USA* **104:** 3777–3781.

Supporting information

Additional supporting information may be found in the online version of this article at the publisher's web-site.